# REACTOR PHYSICS QUARTERLY PROGRESS REPORT AUGUST-OCTOBER, 1953

EDITED BY:

R. A. LAUBENSTEIN



ATOMIC ENERGY RESEARCH DEPARTMENT
NORTH AMERICAN AVIATION, INC.
P. O. BOX 309
DOWNEY, CALIFORNIA

SUBMITTED: DECEMBER 10, 1953

ISSUE DATE

APRIL 15, 1954

CONTRACT AT 11-1-GEN-8

CONFIDENTIAL

REPORT APPROVED BY:

R. A. LAUBENSTEIN, Group Leader, Experimental Physics
A. B. MARTIN, Section Chief, Reactor Physics
S. SIEGEL, Associate Director
C. STARR, Director

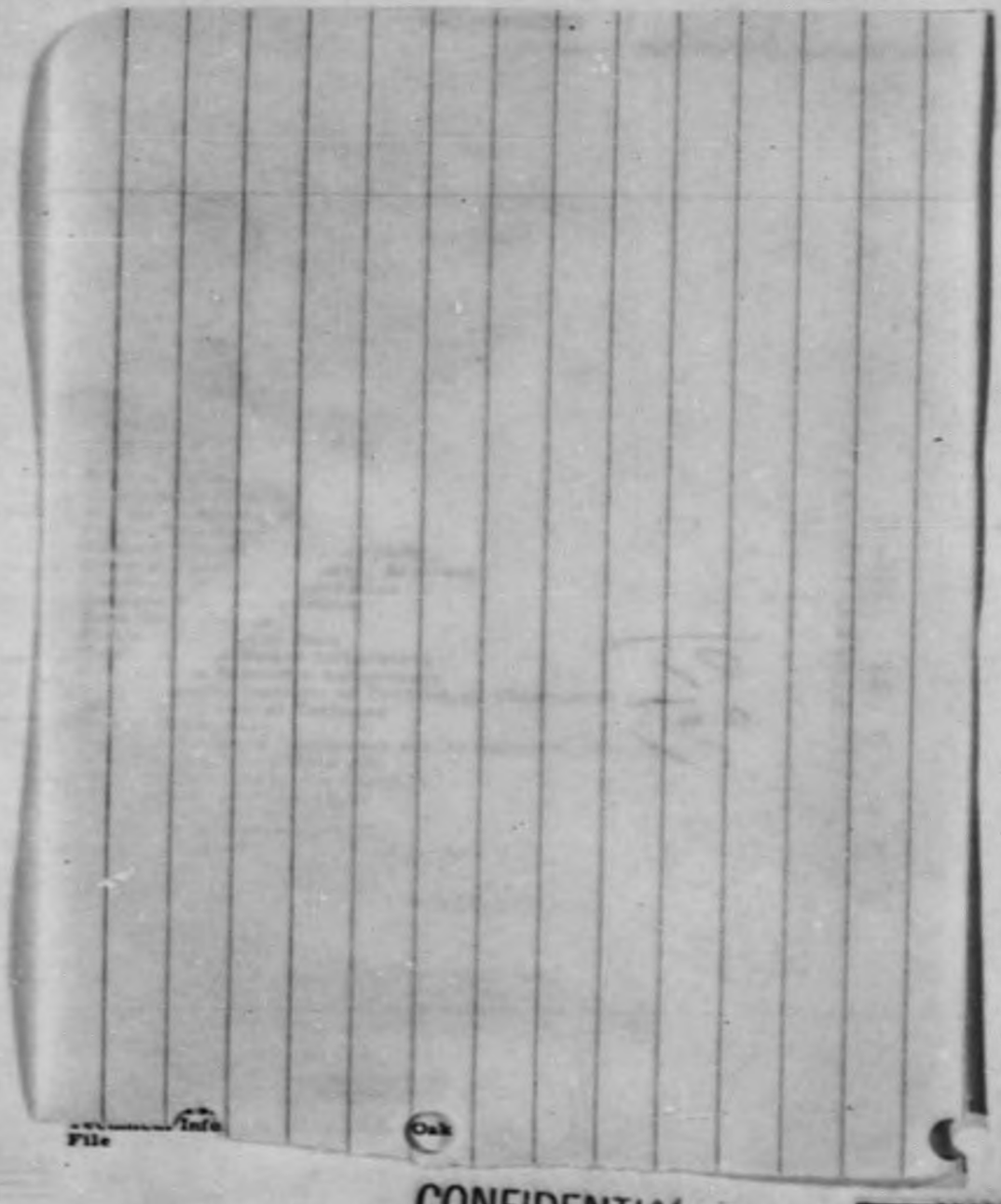

File Info Oak



CONFIDENTIAL

## TABLE OF CONTENTS



## LIST OF TABLES

## LIST OF FIGURES

## ABSTRACT


### Exponential Experiments

Experimental work on the exponential project was resumed during the last two weeks of the quarter after completion of the experimental work on the converter reactor mock-up. A remeasurement of one of the first of 32 "clean" uranium-$D_2O$ lattices investigated at North American Aviation has demonstrated the consistency of the buckling measurements, and of the $D_2O$ purity.

A thorough analysis of the data obtained on depleted, natural, and enriched uranium lattices has been made. Consideration of the possible sources of discrepancies between theory and experiment has led to a suspicion of the calculated thermal neutron diffusion lengths. A series of diffusion length measurements in non-multiplying lattices of lead-cadmium alloy rods has been initiated.

An analysis of some early exponential experiments on lattices proposed for a neutron production reactor has been carried out in order to determine whether experimental results on these more complicated structures are consistent with the analysis carried out for the "clean" lattices.

The possibility of obtaining useful information from an exponential experiment, in which only a single fuel rod is used, has been considered.

A simple numerical method was presented for the analysis of exponential data directly in terms of sinh functions.

### Water Boiler Neutron Source

The use of the WBNS as a facility for measuring neutron absorption cross sections by the danger coefficient technique has been studied further. A calibration of a portion of the coarse control rod has been made in terms of the total absorption cross section of materials placed in the central exposure facility. Danger coefficient measurements on metal slugs of depleted, natural, and slightly enriched uranium indicated that the method could be used as a very sensitive indication of the uranium enrichment.

An automatic control system has been installed on the fine control rod of the WBNS to automatically maintain the reactor at a constant preset power level.

**Theoretical Physics**

A different approach to heterogeneous lattice theory has been applied to slab lattices. An interesting feature of the calculations was the anisotropic effect in these lattices.

This report is based upon studies conducted for the Atomic Energy Commission under Contract AT-11-1-GEN-8.

## I. EXPONENTIAL EXPERIMENTS

### A. Experimental Measurements (S. W. Kash, F. B. Estabrook, B. Engholm)

During most of the quarter, the experimental facilities, which are usually used for the exponential experiments, were used instead for the flux distribution measurements on the mock-up of the converter reactor. Experimental work on the exponential project was resumed during the last two weeks of the quarter.

As a check on experimental procedures in the early part of the exponential experiment program (before the construction of the Water Boiler Neutron Source), and as a simultaneous test of the possibility that our $D_2O$ might have become contaminated during the two years of lattice work, a remeasurement has been made of the buckling of lattice N-1-6 (1 inch diameter natural uranium rods in a 6 inch square lattice). This lattice was one of the earliest lattices which was investigated.

The early value of the buckling for N-1-6 was

$$B^2 = 7.25 \times 10^{-4} \text{ cm}^{-2} .$$

The value now obtained is considerably more accurate because of the greater neutron flux available. The remeasured value is

$$B^2 = 7.22 \times 10^{-4} \text{ cm}^{-2} .$$

The agreement is excellent, and both corroborates the older work and indicates the correctness of our assumption of constant $D_2O$ purity in the lattice calculations based on the accumulated data from some 32 lattices.

### B. Analyses of Depleted, Natural, and Enriched Uranium Lattices in $D_2O$ (F. B. Estabrook, S. W. Kash)

An analysis has been completed of the NAA exponential experiment data on uranium rod lattices in $D_2O$. These data consisted of values of buckling ($B^2$), rod disadvantage factor (F), and moderator disadvantage factor ($F_m$) for some 22 lattices of natural uranium rods, seven of depleted (0.49 per cent)

uranium rods, and three of enriched (0.90 per cent) uranium rods. The data for natural uranium rods has been reported in NAA-SR-138[1] and NAA-SR-209[2]. The more recent data for the depleted and enriched materials can be found in NAA-SR-259[3].

The disadvantage factors have been used to compute, for each lattice, the thermal utilization, f, and diffusion length L. This latter was done by setting $L^{-2} = 3\,\bar{\Sigma}_a\,\bar{\Sigma}_{tr}$, where the bars denote spatial averages over the lattice, weighted with experimental disadvantage factors. The semi-experimental $L^2$ and f, and the experimental $B^2$ were then combined in the two-group criticality equation with computed values of $\eta$ (corrected for effective neutron temperature changes and for reduced epithermal leakage). $\epsilon$ and $\tau$ to give $p_{exp}$, a so-called "experimental" resonance escape probability.

A "theoretical" value, $p_{theo}$, was computed in the usual way by using an effective resonance integral for uranium of 7.3/G + 25.0 S/M. Comparison of $p_{exp}$ and $p_{theo}$ is then a test of both the two-group criticality equation and of this theoretical method of computing p. Since all three enrichments are 99 + per cent $U^{238}$, p is expected to be nearly independent of enrichment.

In Fig. 1, $p_{exp}$ vs $p_{theo}$ is plotted for the 22 lattices of natural uranium rods. The various rod diameters are 0.75 inch, 1.00 inch, 1.25 inches, 1.50 inches and 2.00 inches. In Fig. 2 the same is done for the lattices of depleted and enriched uranium. Definite trends, noted for each enrichment are: (1) the depleted lattices all have $p_{exp}$ about 0.8 per cent high, (2) the natural lattices have $p_{exp}$ about 1 per cent low, (3) the enriched lattices have $p_{exp}$ about 1.6 per cent low. We have made a careful analysis of errors that could contribute to this systematic deviation. Incorrect cross-section values, moderator impurities, etc., could account for only 1/2 per cent spread between the depleted and enriched cases. Hence, we believe our results to be real, and to indicate a real defect in either the two-group theory used in our analysis, or in our assumptions regarding the enrichment and purity of the uranium rods.

In particular, this systematic deviation, which is greatest for lattices with greatest $B^2$, has drawn our attention to $L^2$. If the method of computation of $L^2$ for heterogeneous systems gives results too small by, say, 10 per cent, this would account for the variation of $p_{exp}$ with enrichment. For all these lattices, L is of the same magnitude as the cell spacing, and this makes the

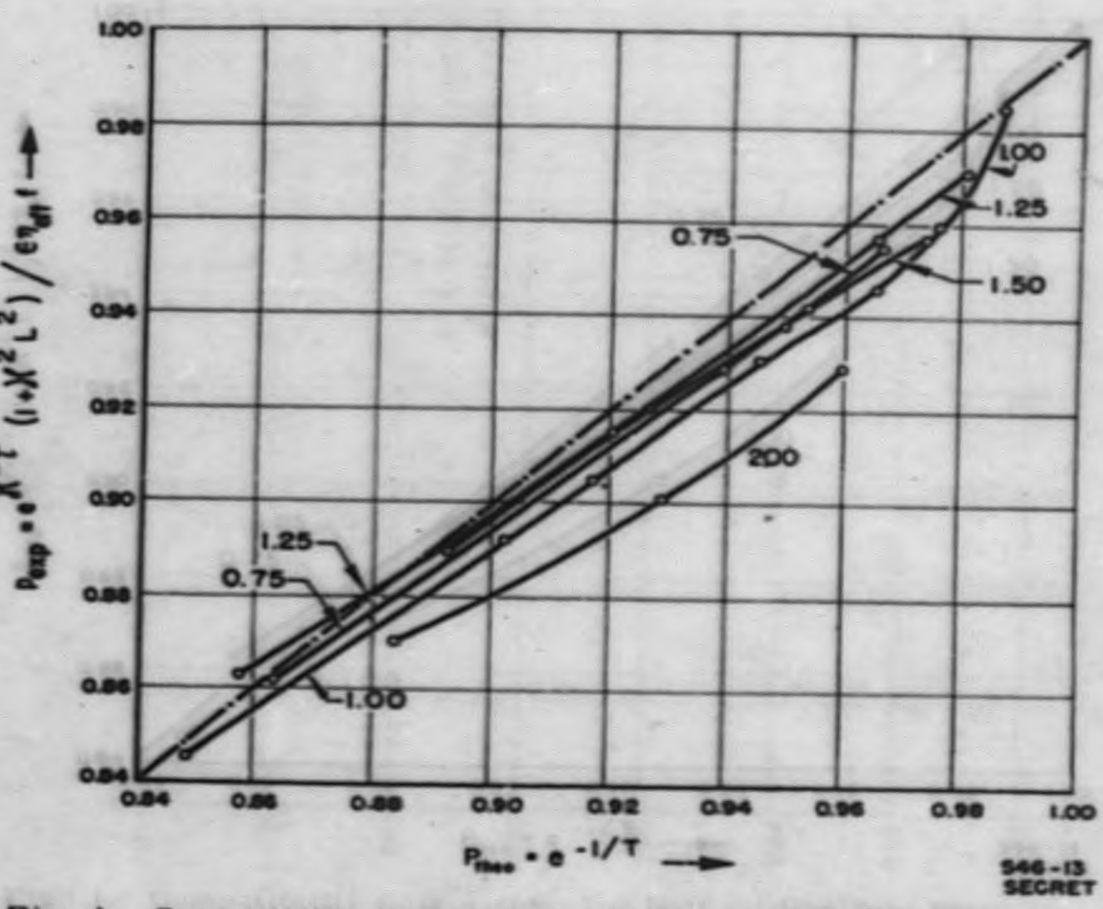


Fig. 1. Compatibility Calculations for Natural Uranium Lattices

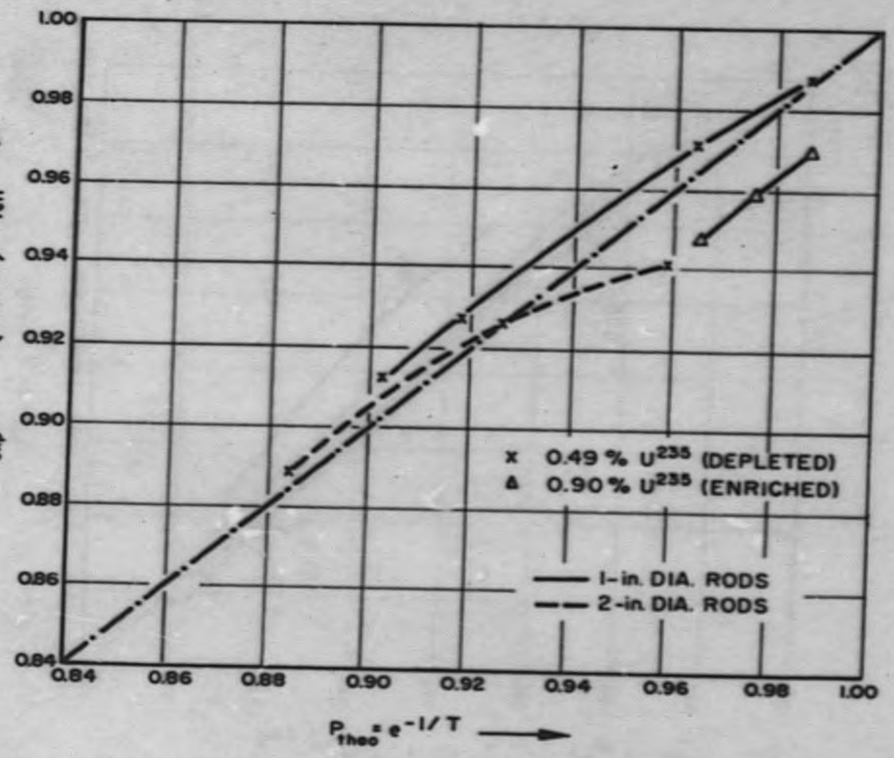


Fig. 2. Compatibility Calculations for Depleted and Enriched Uranium Lattices

usual "homogenization" in the $L^2$ calculation appear uncertain. Again, this raises the possibility that $L^2$ may well be anisotropic. As a result, we have now scheduled a series of experiments on non-multiplying lattices, designed to investigate further the entire question of thermal diffusion lengths in heterogeneous media.

C. Analysis of Neutron Production Reactor Exponential Experiments (E. Martin)

The initial phase of the Exponential Project was intended to supplement the design study of a natural uranium, $D_2O$ moderated, and light water cooled neutron production reactor. These lattices differ from the "clean" lattices discussed in section B above in that they included water and air gaps, and the fuel rods of these lattices contained aluminum discs to simulate the canning of the uranium slugs. These inclusions considerably reduced the experimental bucklings below those of the "clean" lattices. Theoretically, both a smaller f and $\eta_{eff}$ resulted.

Table I summarizes the experimental data available on these lattices. Values of buckling may be somewhat different from those reported in earlier progress reports because of a reanalysis of some of the data. Lack of measured disadvantage factors necessitated the use of diffusion theory in order to calculate thermal utilizations. However, the intra-uranium fluxes and uranium disadvantage factors obtained with the "clean" lattices were used.

An analysis was carried out for the neutron production reactor lattices similar to that discussed in section B above for the "clean" lattices. Results of the calculations are summarized in Table II. If a comparison of the "experimental" with the "theoretical" resonance escape probability is used as a criterion for the validity of the working assumptions, then diffusion theory seems rather inadequate. It has been shown in the analysis of the "clean" lattices that the measured moderator excess absorption exceeds the theoretical value by about 12 per cent. This discrepancy could bring the results of the analysis into correspondence with the analysis of the "clean" lattices.

D. Single-Rod Exponential Experiments (F. B. Estabrook)

In heterogeneous reactor theory, it would be very convenient if the multiplicative properties could be ascribed to the individual lumps of fissile material. In particular, for a rod lattice, such properties could be investigated

## TABLE I

## SUMMARY OF BUCKLING MEASUREMENTS ON NPR LATTICES

| Lattice No. | Fuel Rod Diameter (inches) | Cell Spacing (inches) | Inner Sheath Thickness (inches) | Coolant Film Thickness (inches) | Outer Sheath Thickness (inches) | Air Gap Thickness (inches) | Outer Wall Thickness (inches) | $B^2 \times 10^4$ ($cm^{-2}$) | Flux Ratio R** |
|---|---|---|---|---|---|---|---|---|---|
| 14* | 1.00 | 6.0 | 0.040 | | | | | 7.25 ± 0.07 | 8.4 |
| 3 | 1.00 | 6.0 | | | | | | 6.90 ± 0.10 | 9.3 |
| 4 | 1.00 | 6.0 | | 0.050 | 1/16 | | | 5.59 ± 0.10 | 9.7 |
| 5 | 1.00 | 6.0 | | 0.050 | | 3/16 | 1/16 | 4.55 ± 0.11 | 9.1 |
| 8 | 1.00 | 6.0 | | 0.075 | | | | 4.28 ± 0.11 | 9.5 |
| 10† | 1.00 | 6.0 | | 0.050 | | | | 3.79 ± 0.12 | 9.1 |
| 2 | 0.75 | 6.0 | | 0.050 | | | | 3.15 ± 0.13 | 13.7 |
| 7 | 0.75 | 4.0 | | 0.050 | | | | 3.99 ± 0.12 | 6.1 |
| 9 | 1.25 | 7.25 | | 0.050 | | | | 4.78 ± 0.11 | 9.9 |

*Lattice 14 was a "clean" lattice and contained no aluminum discs between fuel slugs.
†Fuel rod make-up: U slug + Al disc + Cu disc, repeat.
**R = ratio of thermal activation to epicadmium activation for indium foils approximately 90 $mg/cm^2$ thick.

TABLE II

RESULTS OF THEORETICAL CALCULATIONS ON THE NPR LATTICES

| Lattice No. | $\eta$eff | $\epsilon$ | $f$ | $\tau$(cm$^2$) | $L^2$ (cm$^2$) | $P_{theo}$ | $P_{exp}$ |
|---|---|---|---|---|---|---|---|
| 14 | 1.346 | 1.024 | 0.970 | 121 | 193 | 0.945 | 0.931 |
| 3 | 1.342 | 1.022 | 0.968 | 121 | 204 | 0.946 | 0.934 |
| 4 | 1.339 | 1.022 | 0.937 | 115 | 189 | 0.955 | 0.919 |
| 5 | 1.338 | 1.022 | 0.922 | 124 | 191 | 0.952 | 0.912 |
| 8 | 1.337 | 1.022 | 0.908 | 123 | 196 | 0.954 | 0.921 |
| 10 | 1.318 | 1.022 | 0.922 | 125 | 191 | 0.953 | 0.906 |
| 2 | 1.335 | 1.017 | 0.893 | 123 | 292 | 0.970 | 0.936 |
| 7 | 1.337 | 1.017 | 0.911 | 135 | 138 | 0.932 | 0.898 |
| 9 | 1.338 | 1.027 | 0.928 | 122 | 209 | 0.953 | 0.914 |

in an exponential experiment utilizing only one such rod in a tank of the given moderator. This experiment would have the advantage of requiring a minimum amount of critical material.

A two-group calculation has been made for an annular cylinder of $D_2O$, the fluxes being subjected at the outer (extrapolated) boundary (r = a) to the conditions

$$\phi_1(a) = 0$$
$$\phi_2(a) = 0 \qquad \ldots(1)$$

and at the inner boundary (r = b) to the conditions

$$\frac{1}{\phi_2}\left.\frac{\partial\phi_2}{\partial r}\right|_{r=b} = \frac{1}{\delta} \qquad \ldots(2)$$

$$mD_2\left.\frac{\partial\phi_2}{\partial r}\right|_{r=b} = -D_1\left.\frac{\partial\phi_1}{\partial r}\right|_{r=b} \qquad \ldots(3)$$

Equation (2) requires the thermal flux to have an extrapolation length $\delta$ at the rod boundary, and $\delta$ is immediately expressible in terms of the thermal disadvantage factor for the rod. The second condition at the rod boundary has entering thermal current emerge as epithermal-group current multiplied by the factor m.

The result of the calculation is a "criticality equation" for the "axial buckling", $\nu^2$, where, $e^{-\nu z}$ expresses the falling off of all fluxes with the distance, z, up the exponential tank. If $\alpha^2 = 1/L_1^2 - \nu^2$ and $\beta^2 = \nu^2 - 1/L_2^2$, this result is

$$m\frac{L_2^2}{L_2^2 - L_1^2} = \frac{Q(\beta) - \delta}{Q(\beta) - \bar{Q}(\alpha)} \qquad \ldots(4)$$

where

$$Q(x) = \frac{1}{x} \frac{J_o(ax)\, Y_o(bx) - J_o(bx)\, Y_o(ax)}{J_o(ax)\, Y_o'(bx) - J_o'(bx)\, Y_o(ax)} \quad . \qquad \ldots(5)$$

and the definition of $\bar{Q}$ differs only in that $I_o$ replaces $J_o$, and $K_o$ replaces $Y_o$. These functions are zero order Bessel functions. The primes denote differentiation with respect to the argument.

When m is plotted vs $\nu$ it appears that, for rod sizes of interest, since $\delta$ can easily be determined (from radial traverses) to 0.1 centimeter, an accuracy of about ± 0.5 per cent in $\nu$ would suffice to determine m to ± 2 per cent.

E. A Simplified Method for the Analysis of Exponential Flux Data (S. W. Kash)

A numerical method has been developed for the rapid analysis of exponential pile flux data. The method can be applied in cases where the data are to be fitted to two or more sinh functions. The computations involved are extremely simple, and are relatively free of bias. The reciprocal relaxation lengths are determined directly from the data without the necessity of obtaining normalization constants or extrapolation distances.

In the usual situation, where a single sinh or exponential function fit is adequate, the analysis is particularly simple. In this case the data, $y(z_m)$, are arranged into three groups from which we may form sets of three equally spaced points, $y(z_m - p)$, $y(z_m)$ and $y(z_m + p)$. We then obtain the average of the quantities $q = \left[ y(z_m - p) + y(z_m + p) \right] / 2y(z_m)$ for the sets thus formed. The reciprocal relaxation length is then obtained directly by the relation

$$\nu = \frac{1}{p} \cosh^{-1} \bar{q} \quad .$$

Some care should be exercised in the grouping of the points. It is desirable to take p large so as to decrease the sensitivity of $\nu$ to errors in q, but not so large as to waste measured data. In any particular case, the division would depend upon the value of $\nu$, the amount of data, and the positioning of and the weight attributed to the data. A reasonable compromise in many cases, where the data is equally spaced and about of equal weight, is to put the first third

of the data into one group, the second third into another group and the remainder into the third group.

For a double sinh fit, the procedure is somewhat more complicated. The data must now be grouped into sets of five equally spaced points. . For each set of points we then form the quotient pairs:

$$q' = \left[ y(z_m - p) + y(z_m + p) \right] \Big/ 2y(z_m) \text{ and } q'' = \left[ y(z_m - 2p) + y(z_m + 2p) \right] \Big/ 2y(z_m).$$

From these, the auxiliary functions $w_1$ and $w_2$ are obtained, where

$$w_1 - 2q' w_2 + q'' = 0 \quad .$$

These in turn determine the two reciprocal relaxation lengths by the relation

$$\nu = \frac{1}{p} \cosh^{-1} \frac{1}{2} \left[ w_2 \pm \sqrt{w_2^2 - 2w_1 + 2} \right]$$

F. Solutions for the Two-Region, Two-Group Problem with Streaming: Cylindrical Geometry (S. W. Kash)

To investigate the merits of using reflected assemblies for exponential experiment work, diffusion solutions were obtained for a two-region, two-group neutron problem. Concentric cylindrical regions were chosen, and net neutron currents in the axial direction were assumed. The general solution for each flux in the central region is then of the form

$$\sum_{\nu_n} R_n(r) \left( A_n e^{\nu_n z} + B_n e^{-\nu_n z} \right) \quad . \qquad \ldots(6)$$

where $R_n(r)$ is the sum of two zero order Bessel functions. Assuming that the multiplication constant k is greater than one in the central region, then

$$R_n(r) = a(\nu_n) J_o(\mu_1 r) + b(\nu_n) I_o(\mu_2 r) \quad . \qquad \ldots(7)$$

for small values of $\nu$ and

$$R_n(r) = a(\nu_n) I_o(\mu_1 r) + b(\nu_n) I_o(\mu_2 r) \quad . \qquad \ldots(8)$$

for large values of $\nu$. The $\mu$'s are given by the relation

$$\mu_i = \sqrt{|\nu^2 + B_i^2|} \quad . \qquad \ldots(9)$$

where the two bucklings $B_i^2$ are obtained from the usual two-group compatibility equation

$$(1 + B^2 L^2)(1 + B^2 \tau) = k \qquad \ldots(10)$$

The values of $\nu^2$, and the corresponding constants $a(\nu)$ and $b(\nu)$, must be determined from the properties and radial dimensions of the two media. The constants $A_n$ and $B_n$ depend upon boundary conditions at the ends of the cylinder. In case the smallest value, $\nu_1^2$, is negative, it is preferable to replace the exponentials $e^{+\nu_1 z}$ by the sine and cosine of $\nu_1 z$.

In many cases, the solution is adequately approximated by the first element of the series Eq. (6). Furthermore, in this case, the $J_o$ term in Eq. (7) usually dominates over the central portion of the inner cylindrical region.

For exponential experiments, such a double region arrangement appears undesirable. Aside from the greatly increased criticality hazard, it would be extremely difficult to measure accurately the material buckling of the inner medium or lattice. This would be given by the usual relationship, $B_1^2 = \mu_1^2 - \nu^2$, where $\nu^2$ is the asymptotic or smallest value. The vertical buckling $\nu^2$ could still be measured accurately, but the radial buckling $\mu_1^2$ would have a large uncertainty in it. The behavior of the Bessel function $J_o(\mu r)$ is such that the determination of $\mu$ is most sensitive to flux measurements near the edge of the inner region. However, it is here that the $I_o$ term contributes most to the flux. Here also, uncertainties arising from irregular lattice cell structure at the boundary are greatest. Because of the limitations imposed by the cell structure on the number of radial measurements that can be made, and because of the usual inaccuracies of flux measurements, it is difficult to get a definitive fit to the two Bessel function formula, $a J_o(\mu_1 r) + b I_o(\mu_2 r)$.

Separating the two regions by a cylindrical sheet of cadmium simplifies the computations necessary to determine $\nu$, $a(\nu)$ and $b(\nu)$. However, the radial form of the solution for the inner medium is unchanged; hence, the objections raised in the preceding paragraph are also applicable to this modified arrangement.

## II. WATER BOILER NEUTRON SOURCE

During the months of August, September, and October, the Water Boiler Neutron Source was operated for a total of 273 watt-hours of which approximately two watt-hours were service irradiations, seven were danger coefficient measurements, and the remainder were for the converter reactor mock-up and exponential experiments.

### A. Danger Coefficient Measurements (M. E. Remley, D. C. Woods)

1. Calibration of the Coarse Control Rod - The use of the WBNS as a facility for measuring neutron absorption cross section with the danger coefficient technique has been studied further. A calibration of a portion of the coarse control rod of the reactor has been made in terms of the total absorption cross section of materials placed in the central exposure facility. This calibaration will enable future absorption cross section measurements to be made in terms of control rod position.

The calibration was performed using standard samples in the form of specially prepared wafers of boron impregnated bakelite. The experimental techniques are those described briefly in a previous progress report.[4] The results of the calibration experiments are given in Fig. 3 in the form of a curve of $\frac{\Delta\Sigma}{\Delta\chi}$ versus rod position, $\chi$, where $\Sigma$ is the total neutron absorption cross

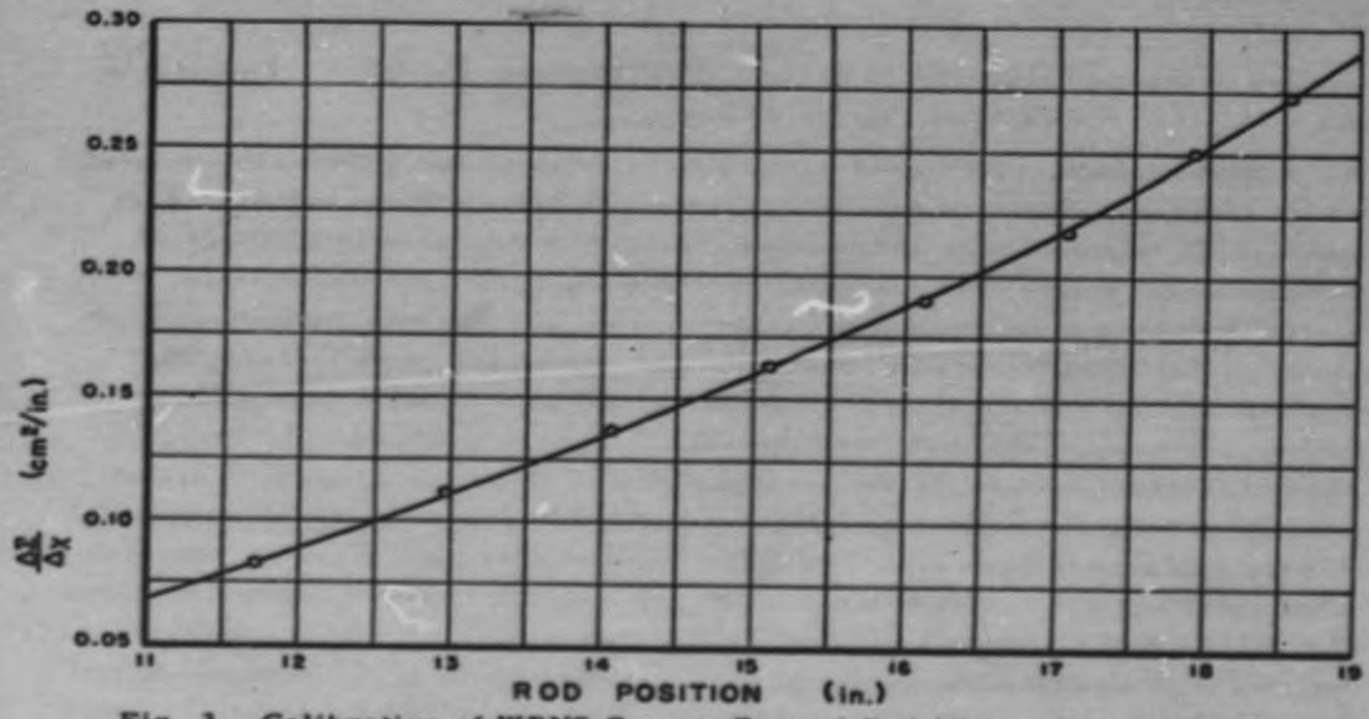


Fig. 3. Calibration of WBNS Coarse Control Rod (Cross Section per Unit Rod Movement vs Rod Position)

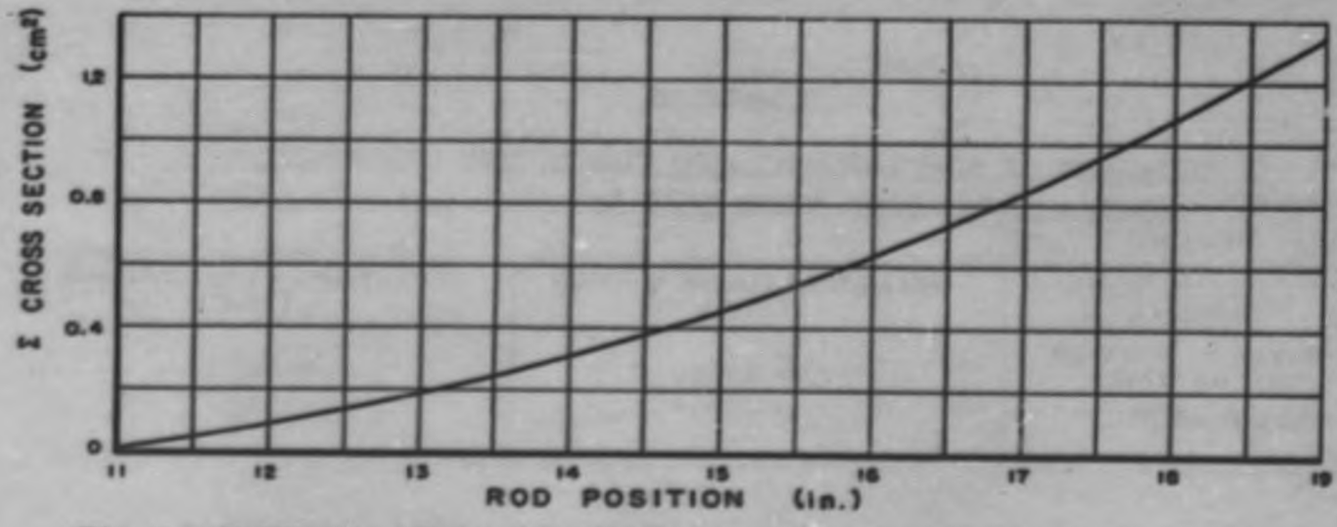


Fig. 4. Calibration Curve for WBNS Coarse Control Rod (Cross Section vs Rod Position)

section of the materials placed in the central exposure facilities. Figure 4 is the integral of the curve of Fig. 3, or $\Sigma$ vs $\chi$.

Experiments, which were performed in order to check the absolute value of the ordinate of these curves, included a measurement of the thermal cross section of a thin gold foil, and the cross section of the boron in a sample of borated heavy water. The thermal cross section of the gold was obtained from the difference of a measurement on the bare foil and one with the foil cadmium covered. The results of these measurements, which are given in Table III, indicate that the standard boron impregnated bakelite samples have a lower boron content than was calculated from the method of preparation. The measured cross section for the borated $D_2O$ was 18 per cent higher than that calculated from the boron concentration of the solution, while the discrepancy for the gold was 12 per cent. The discrepancy for the gold becomes even higher when (qualitative) account is taken of the fact that the cadmium correction takes out the tail of the 1/v, absorption as well as resonance absorption. Although borated $D_2O$ was directly compared with pure $D_2O$ in the measurements on the boric acid solution, some error may have been introduced by a possible change in neutron energy distribution or statistical weight of the exposure facility caused by the moderating effects of the $D_2O$.

TABLE III

RESULTS OF EXPERIMENTS TO CHECK THE STANDARD SAMPLES USED FOR WBNS CONTROL ROD CALIBRATION

| Sample | Measured Cross Section ($cm^2$) | Calculated Cross Section ($cm^2$) |
|---|---|---|
| Boron in Borated Heavy Water | 0.0315 | 0.0267 |
| Thin Gold Foil | 0.171 | 0.1527 |

A continuing effort is being made to obtain accurate standard samples, as well as to study other effects which might contribute to the observed discrepancies.

2. Danger Coefficient Measurements on Metal Slugs - Danger coefficient measurements have been made to determine effective (effect on WBNS reactivity) cross sections of several metal slugs compared with natural uranium. Samples used were as follows:

(1) Natural uranium
(2) Depleted uranium (0.49 per cent $U^{235}$)
(3) Enriched uranium (0.90 per cent $U^{235}$)
(4) Thorium
(5) Lead

All samples were machined to 0.750 inch diameter by 1.000 inch long with tolerances of ± 0.002 inch.

Danger coefficient measurements were made in the usual manner, comparing natural uranium with each of the other slugs and obtaining a difference in effective cross section by means of the calibrated control rod. The results of these measurements are shown in Table IV. The last column of this table shows the increase in effective cross section per atom over that of natural uranium.

Figure 5 is a plot of the cross section difference from natural uranium vs $U^{235}$ content. The departure from linearity is to be attributed to greater self-shielding in samples with greater $U^{235}$ content. Assuming a sensitivity of $10^{-3}$ $cm^2$ for the danger coefficient technique, it may be seen that the $U^{235}$

TABLE IV

DANGER COEFFICIENT MEASUREMENTS ON METAL SLUGS

| Sample | Weight (gm) | $\Sigma$(sample) - $\Sigma$(natural U) ($cm^2$) | No. of Atoms x $10^{-23}$ | $\Delta\sigma_{eff}$ (barns) |
|---|---|---|---|---|
| Depleted Uranium | 137.10 | 0.197 | 3.467 | 0.568 |
| Enriched Uranium | 137.24 | -0.158 | 3.470 | -0.455 |
| Thorium | 84.48 | 1.158 | 2.191 | 5.285 |
| Lead | 81.92 | -0.110 | 2.380 | -0.462 |

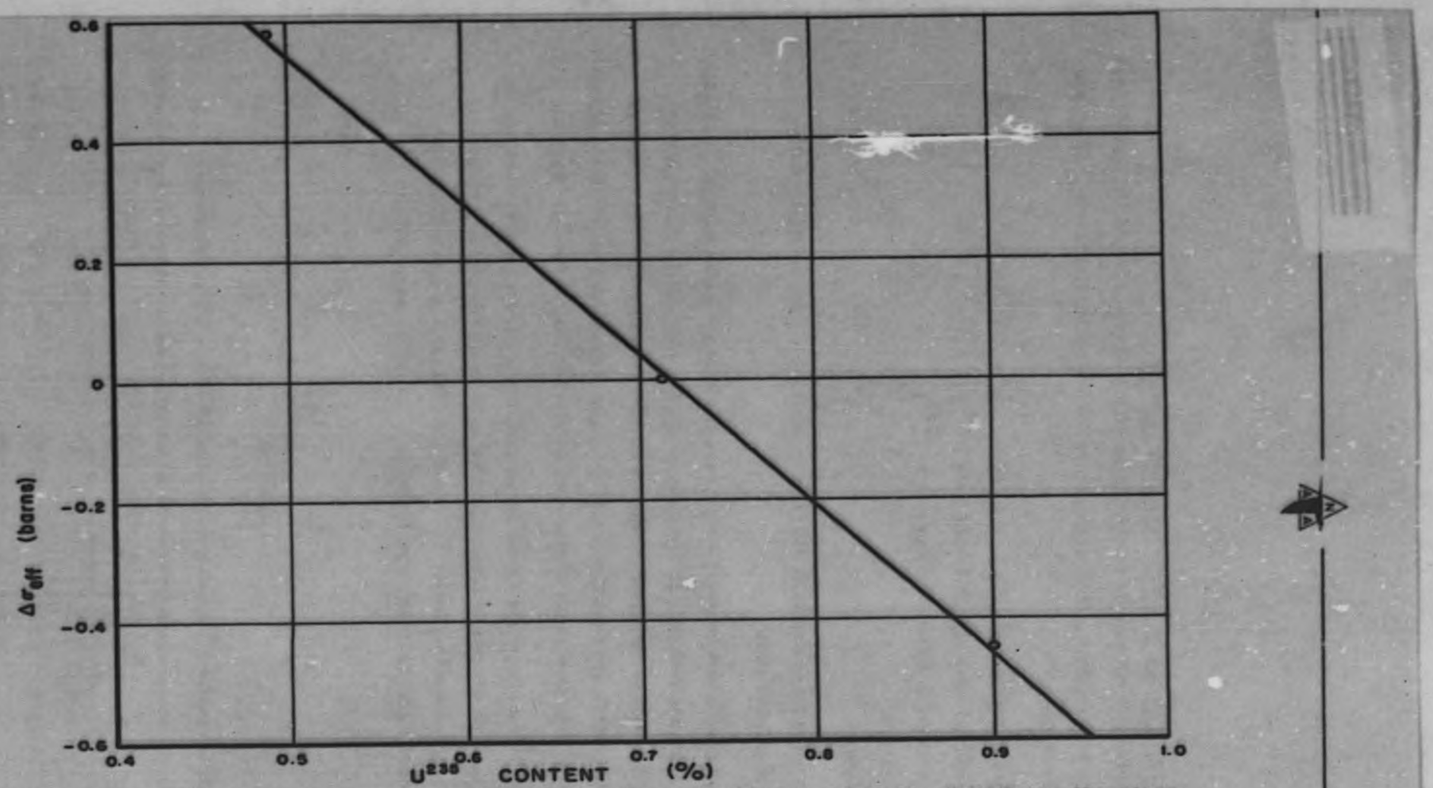


Fig. 5. Effective Microscopic Absorption Cross Sections Measured in the WBNS for Uranium with Different Enrichments of $U^{235}$

content of a sample of pure uranium (with $U^{235}$ content of this order) may be determined by this method to within 0.0012 per cent using slugs of about 137 grams weight. Better accuracy could be obtained with larger slugs.

B. Automatic Control for the WBNS (D. C. Woods)

An automatic control has been installed on the WBNS to continually adjust the fine control rod so as to maintain a constant preset power level. A Brown recorder amplifier is so arranged that its input is the difference between the voltage from a power set potentiometer and the output of a vibrating reed electrometer which amplifies the output of an ion chamber. The amplifier output drives a two-phase A. C. motor. (A Brown recorder chart drive motor was used.)

In this way, the fine rod is driven faster, the greater the difference between actual and desired water boiler power. Provision is made for switching to manual control when desired. If, while on automatic control, the fine rod reaches either end of its travel, a buzzer sounds to warn the operator that manual control is required.

## III. THEORETICAL PHYSICS

A. Heterogeneous Lattice Theory (F. B. Estabrook)

The usual approach to heterogeneous lattice reactors is to treat them as homogeneous media with both moderating and multiplying properties. For example, one could use suitable averages for quantities such as $\Sigma_1$, $D_1$, $L_1$, $\Sigma_2$, $D_2$, and $L_2$ (1 and 2 referring respectively to epithermal and thermal neutrons), and then apply the two-group diffusion theory applicable to a uniform multiplying medium. This "homogenization" is obviously open to objection, as what constitutes a "suitable average" is often not clear, and also as anisotropic effects in the diffusion are thereby automatically neglected.

It is proposed that the application of the theory of neutron moderation and diffusion to only the multiply connected moderator portion of the reactor obviates the above difficulties. The other half of the reactor picture, the multiplication provided by lumped fissile material, then appears in multiplying-boundary conditions to be applied to the diffusion problem.

As a first application of these ideas a lattice of parallel uranium slabs (thickness $d = \ell$, spaced $\ell$ apart) was considered. Two-group non-multiplying diffusion theory was applied to the moderator volumes between the slabs, subject to the following boundary conditions: (1) epithermal continuity through the slabs, (2) thermal extrapolation length $\epsilon$, and (3) net thermal current into a slab emerges, multiplied by m, as epithermal current. The criticality equation that results gives indirectly the gross or large-scale buckling $\mathcal{B}^2$ of the lattice:

$$\cos \mathcal{B}d = \frac{\frac{L_1}{L_2}\left[\cosh\frac{\epsilon}{L_2}\sinh\frac{\epsilon}{L_1} + \cosh\frac{\epsilon+\ell}{L_2}\sinh\frac{\epsilon+\ell}{L_1}\right] - K\sinh\frac{2\epsilon+\ell}{L_2}\cosh\frac{\ell}{L_1}}{\frac{L_1}{L_2}\left[\cosh\frac{\epsilon}{L_2}\sinh\frac{\epsilon+\ell}{L_1} + \cosh\frac{\epsilon+\ell}{L_2}\sinh\frac{\epsilon}{L_1}\right] - K\sinh\frac{2\epsilon+\ell}{L_2}} \qquad \ldots(11)$$

where $K = 1 - \frac{D_1}{\Sigma_{1m}}\left(\frac{1}{L_1^2} - \frac{1}{L_2^2}\right)$ .

Anisotropic effects can be investigated by replacing $1/L_1$ in Eq. (11) by $\frac{i}{L_1'} = \sqrt{\frac{1}{L_1^2} + \nu^2}$ , $1/L_2$ by $\frac{1}{L_2'} = \sqrt{\frac{1}{L_2^2} + \nu^2}$ , and $\mathcal{B}$ by $\mu$.

$\mu^2$ is then the longitudinal buckling (i.e., normal to the plates) and $\nu^2$ the transverse buckling. The "homogenized" one-group anisotropic criticality relation

$$\frac{\mu^2}{(k-1)/M_\perp^2} + \frac{\nu^2}{(k-1)/M_\parallel^2} = 1 \qquad \ldots(12)$$

shows that a plot of $\mu$ vs $\nu$ would be elliptical if the transverse and longitudinal migration areas $M_\perp$ and $M_\parallel$ respectively, are not equal.

For a sample calculation of the anisotropic effect, $d = \ell$, or the slab thickness, was chosen as 2.54 centimeters. Data taken at NAA gives the extrapolation length to be $\epsilon = 2.92$ centimeters for these 1 inch natural uranium slabs. Other

values used were m = 1.35, $L_1$ = 11 centimeters and $L_2$ = 100 centimeters. Equation (11) gave a pronounced maximum value of $\gamma\ell$ of 0.04 centimeter$^{-1}$ at L≅ 13 centimeters. At separations greater than $\ell$ ≅110 centimeters, criticality appears impossible. For the optimum case of $\ell$ ≅13 centimeters, the anisotropy calculation gives results as shown in Fig. 6. The curve of $\mu$ vs $\nu$ is indeed very closely elliptical, and in conjunction with Eq. (12) gives

$$\frac{M_\perp{}^2}{M_\parallel{}^2} = 1.27 \quad .$$

**B. Gamma Activity from Fission Product Chains Containing Volatile Elements**
(R. L. Ashley)

There is an abundance of information in the literature dealing with gamma radiation from fission products. Most of this data suffers, however, from a lack of information on two important points: (a) radiation levels at cooling times shorter than one day; (b) separation of gamma ray intensities according to the energy of the gamma rays. In the design of a gas handling system for water boiler reactors, it was considered desirable to have some estimates of the gamma activity which one might encounter in the unit, and the shielding required, for cooling times of the order of hours or minutes.

It was decided, therefore, to utilize the method of Thornton and Houghton[5] and construct an influence function for the hard gamma emitters in fission products. Briefly, this method (with regard to beta activity) is to obtain the influence function $\beta(t)$, the activity of all fission product nuclei at time t, per unit fission of $U^{235}$ at time t = 0. Extending the fission process over a finite period of time, and letting this time, which is denoted by $\tau$, extend from $-\infty$ to 0 (and t from 0 to $+\infty$), the total beta activity of the fission products, $C(\tau, t)$, is

$$C(\tau, t) = \int_\tau^0 \beta(t - \tau') \cdot R(\tau')\, d\tau' \quad ,$$

where $R(\tau')$ is the fission rate. Substitution of $a = t - \tau'$ gives

$$C(\tau, t) = \int_t^{(t-\tau)} \beta(a) \cdot R(t - a)\, da$$

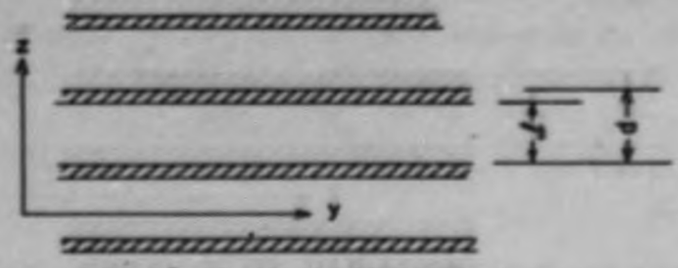


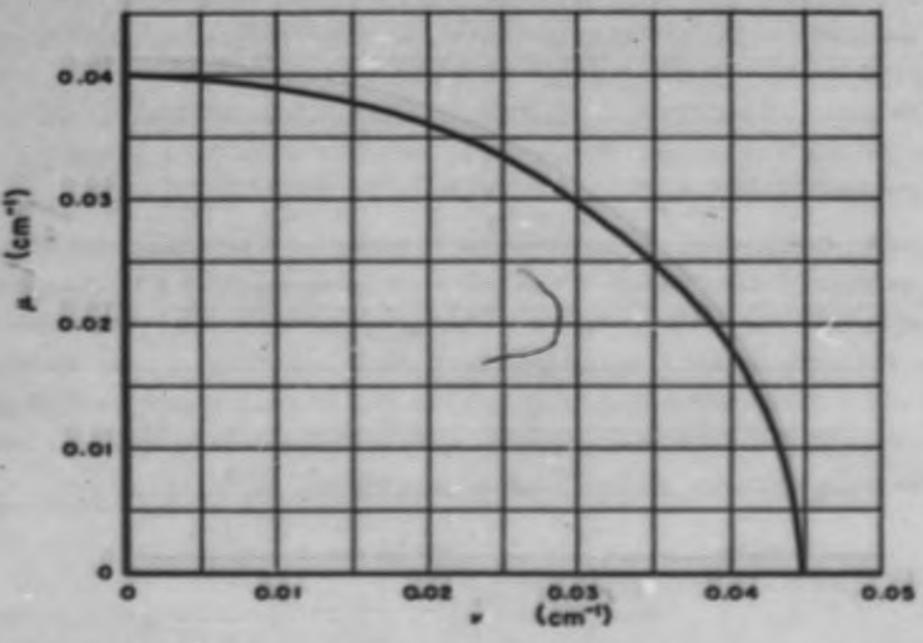


Fig. 6. Longitudinal vs Transverse Buckling for a Slab Lattice

and, if the fission rate is constant during the period of exposure,

$$\frac{C(\tau, t)}{R} = \int_t^{(t-\tau)} \beta(a)\, da \quad .$$

where C/R is the beta activity at time t, per unit constant fission rate. Plotting the integral $\int_o^t \beta(a)\, da$, the activity per unit fission rate is found by simply taking the difference of the two ordinates at $t - \tau$ and t. (Note that $\tau$ is a negative number.)

The problem, as to what isotopes to use in the gamma radiation analysis, was resolved by considering all volatile elements and descendants of these elements, which occur as fission products or in fission product decay chains. The volatile elements considered were bromine, krypton, tellurium, iodine and xenon. All isotopes emitting gamma rays of energy less than 1 Mev were neglected, since lead was to be used as shielding material. The isotopes selected were: Rb-88, Sr-91, Y-94, Te-131, Te-133, I-132, I-133, I-134, I-135, Cs-138, Ba-139, La-140, and Pr-144. The decay schemes used are shown in Fig. 7. Five other isotopes emitting gammas harder than 1 Mev were not considered (Br-87, Kr-89, Rb-86, Y-92, and I-136). They were eliminated due to either short half-life or low fission yield.

Using these 13 isotopes, the curve in Fig. 8 was obtained. This curve shows the influence function $\Gamma(t)$ vs the time (t). To obtain the curve of

$$\int_o^t \Gamma(a)\, da \quad ,$$

it is only necessary to integrate the curve of Fig. 8. This has been done and the resultant curve plotted in Fig. 9. One qualification should be made regarding this latter figure, namely that the lower limit of the integral

$$\int_o^t \Gamma(a)\, da$$

is not defined by Fig. 8. However, as long as $\tau$ is large, say at least 60 minutes, the error is quite small.

## $Rb^{88}$

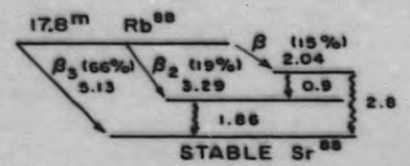


NOTE: In this analysis we assumed that $\beta$ is always followed by the 2.8 Mev $\gamma$.

## $Y^{94}$

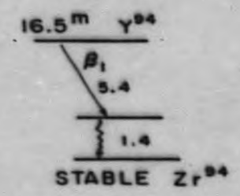


## $I^{132}$

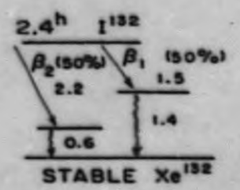


NOTE: In this analysis we include a 2.0 Mev $\gamma$ in 2.7% of the disintegrations.

## $Sr^{91}$

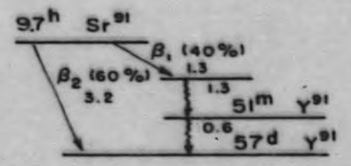


## $Te^{131}$

22% of decays accompanied by a 2.2 Mev $\gamma$.

## $I^{133}$

1% of decays accompanied by a 1.4 Mev $\gamma$.

## $Te^{133}$

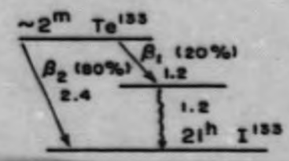

$I^{134}$

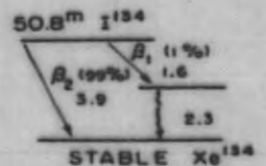


$Cs^{138}$

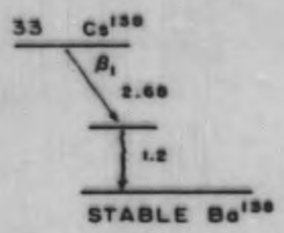


$La^{140}$

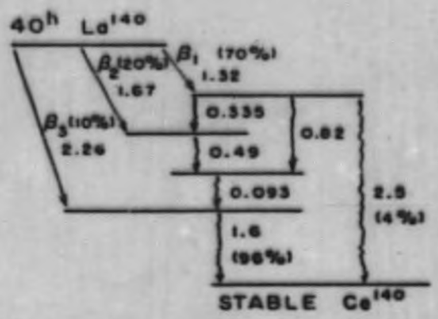


$I^{135}$

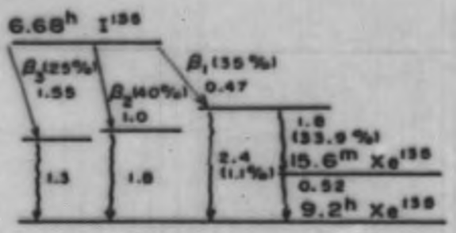


$Ba^{139}$

0.6 % of decays accompanied by a 1.05 Mev $\gamma$.

$Pr^{144}$

3 % of decays accompanied by a 2.2 Mev $\gamma$.



Fig. 7. Decay Scheme of Hard Gamma Emitters

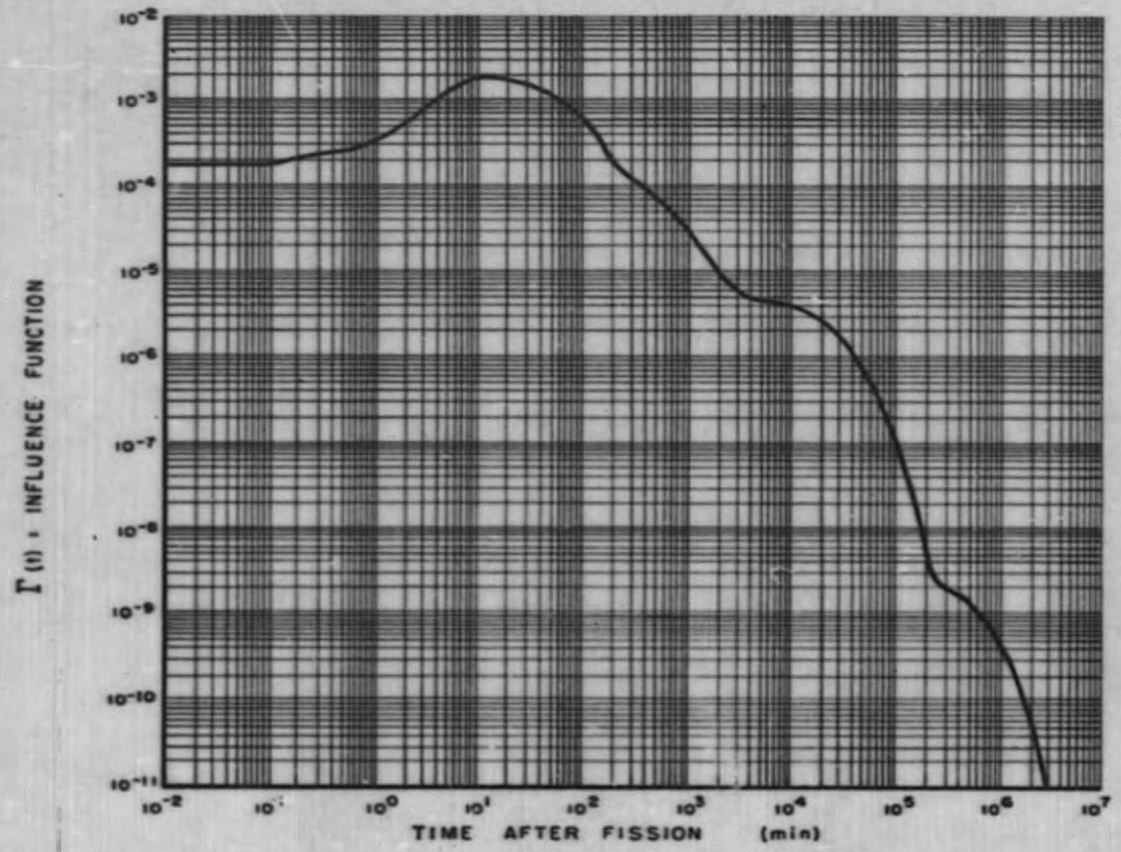


Fig. 8. The Influence Function of the Hard $\gamma$ Emitters in Effluent Gas

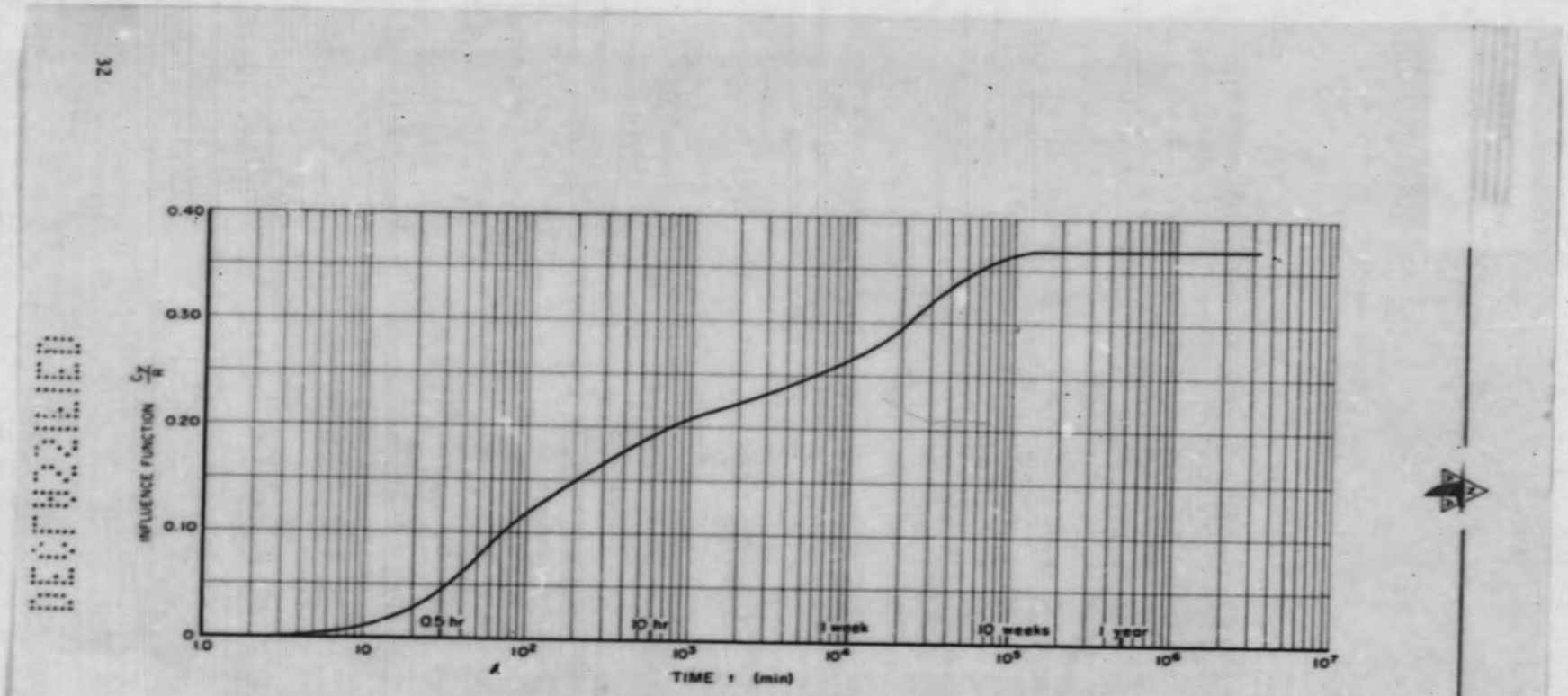


Fig. 9. An Integral Curve of the Influence Function vs Time after Fission

From Fig. 9, for long irradiation periods ($>3 \times 10^5$ min $\approx$ 200 days), at a constant power level of 100 watts, the hard gamma activity in the volatile fission products and their descendants, 30 minutes after shutdown, amounts to 27 "curies" where the "curie" is defined as that amount of material which emits $3.7 \times 10^{10}$ gamma rays per second. Analysis of the spectral distribution indicates that the average gamma ray energy is about 2.0 Mev.

## REFERENCES


1. Woods, D. C. and A. T. Biehl, "Intra-Cell Neutron Densities in Natural Uranium-$D_2O$ Lattices, Part II," NAA-SR-138, Part II, August 4, 1953.
2. Kash, S. W., "Buckling Measurements of Thermal Neutrons in Natural Uranium-$D_2O$ Square Lattices," NAA-SR-209, February 12, 1953.
3. Laubenstein, R. A., "Reactor Physics Quarterly Progress Report for February - April, 1953," NAA-SR-259, October 1, 1953.
4. Laubenstein, R. A., "Reactor Physics Quarterly Progress Report for May - July, 1953," NAA-SR-275, March 1, 1954.
5. Thornton, J. K. and W. J. Houghton, "An Influence Function for the Beta Activity of Uranium (235) Fission Products," NAA-SR-45, September 1, 1950.






END